Simple All-Inorganic Electroluminescent Devices Based on Type-II CdTe/CdS/ZnS Core/Shell/Shell Quantum Dots

A, Watts[(1)] , A. Waheed[(1)] , and M. Green[(2)]

.

(1) British Institute of Technology & E-commerce (BITE), Avicenna House,258-262 Romford Road, London E7 9HZ, United Kingdom
Email: waheed {at} bite.ac.uk

(2) Department of Physics, King's College, Strand, London WC2R 2LS, United Kingdom

ABSTRACT--- ***The purpose of this work is to investigate the basic electrical properties of type –II CdTe/CdS/ZnS core/shell/shell quantum dot to explore the use in all- inorganic light emitting diodes towards the application in optoelectronic devices. It was based on the development of colloidal quantum dots consisting of semiconductor nanocrystals which provided potential electroluminescence devices. The use of nanocrystals allows the emission wavelength to be tuned to cover a wide range of wavelengths. Suggestions have been given for the future research in this direction.***

Keywords-- Quantum dot heterostructures, Nanocrystalline semiconductors, Inorganic light emitting devices (LEDs) , Optoelectronic devices

1. INTRODUCTION

Nanocrystalline semiconductors are the attractive materials for light emitting sources due to their high quantum efficiencies, narrow line-like emission and tuneability across the visible & near infrared regions of the spectrum. The similar studies carried out recently included using different methods in the fabrication of nanocrystals (1-5). To date, however, there have been relatively a few reports about the quantum dots-based all-inorganic light emitting structures containing type-II core/shell/shell quantum dot heterostructures of CdTe/CdS/ZnS . The emission profile in unchanged and demonstrates that core/shell/she// structures based on aqueously prepared CdTE quantum dots have the potential for practical devices. Semiconductor quantum dots (QDs) are attractive due to their size quantization which manifests itself in size dependent changes in the optical and electrical properties (6,7). In colloidal quantum dots, the optical and electronic properties are determined by the quantum confinement effect (8), which is due to the physical confinement of bulk material through carefully controlled chemical reactions (9). Moreover, the ease of processing nanocrystals is an advantage in the low cost fabrication of devices via spin casting.

A number of different structures, which make use of semiconductor QDs as a light emitting material, have been investigated by several groups (6,10). There are three main types of LEDs based on quantum dots, namely (i)self-assembled(11-13), (ii) colloidal-all inorganic devices in which the active layer comprises a neat film of the emissive dots, and (iii) hybrid organic-inorganic devices in which the dots are dispersed in a host organic semiconductor matrix. . The first hybrid LEDs used cadmium selenide (CdSe), but they had low external quantum efficiencies (EQEs) of between 0.001 and 0.01% and the maximum luminosities of only 100 cd/m , although subsequent optimization of the device architecture enabled the external quantum efficiencies to reach 0.1%.The device structures improved gradually until a new device architecture was reported by Coe et al (21) in which a monolayer of CdSe/ZnS dots, formed by spontaneous phase segregation, was sandwiched between two organic thin films, with external quantum efficiency of up to 1.1%. The improved performance of these monolayer-based devices was attributed to an improved balance of electron and hole injection, a major stumbling block previously in the hybrid devices. The CdTe particles, prepared earlier by aqueous chemistry and capped with simple thiols ligands alone, have been used in hybrid LEDs and in all-inorganic devices. This was advanced further using CdTe particle layers sandwiched between Indium Tin Oxide (ITO) and aluminium electrodes deposited by vapour deposition, giving EQE of up to 0.5% in the best possible case. The use of core/shell particles appears to offer longer device stability, as the shell layers offer protection to oxidation. The carrier transport properties can give information of the density of the trapping level in thin-film device structures made of QD composites (14) or conjugated polymers (15), which have been well characterised using space-charge limited models. The purpose of this work is to characterise the electrical and optical properties of CdTe/CdS/ZnS core/shell/shell on different substrates for application to optoelectronic devices(16).

We in this work have explored the possible use of aquously prepared CdTe/CdS/ZnS quantum dot structures to prepare a simple all-inorganic light emitting device. CdTe is an important II-VI semiconductor quantum dot because of its large exciton Bohr diameter measuring 15 nm (12). We have used a recently developed extension of the route where several shell layers are deposited onto the emitting core to give a type II structure (CdTe/CdS/ZnS core/shell/shell). To our knowledge the type II quantum dots have not been used in the light-emitting devices preparation. The purpose of this work is to explore the feasibility, and characterise the electrical & optical properties of CdTe/CdS/ZnS core/shell/shell QDs on different substrates for application to optoelectronic devices, and compare the results with other devices (17-20).

2. EXPERIMENTAL METHOD

The CdTe quantum dots were prepared by a 'one pot' route (16) . The optical absorption and the photo-luminescent studies were performed on thin film deposited by spin coating over the spectrosil B disks. The device structure consisted of an emissive CdTe nanocrystal layer sandwiched between (ITO) and a thermally evaporated calcium cathode capped with aluminium at base pressure of approximately 10^{-6} mbar. The anode hole injection performance is improved by depositing poly-(ethylene dioxythiophene) doped with poly-styrene sulfonic acid (PEDOT:PSS) onto ITO that has been pre-treated with oxygen plasma at 10 W for 5 min.

The CdTe was deposited by either drop casting or spin coating from a solution. Multilayered devices with either CdTe and F8BT [poly(9,9-dioctylfluorene-alt-benzothiadiazole)], or CdT were also prepared. The devices were tested at a vacuum of 10^{-2} mbar.

3. RESULTS AND DISCUSSION

Absorption and emission spectra for CdTe in solution/solid are shown in Figure 1, with an absorption edge at about 430 nm. Due to the size restriction, the absorption spectrum in the bulk shifts by more than 1 eV, from 827 nm in CdTe crystal to 400-500 nm in the clusters (22).

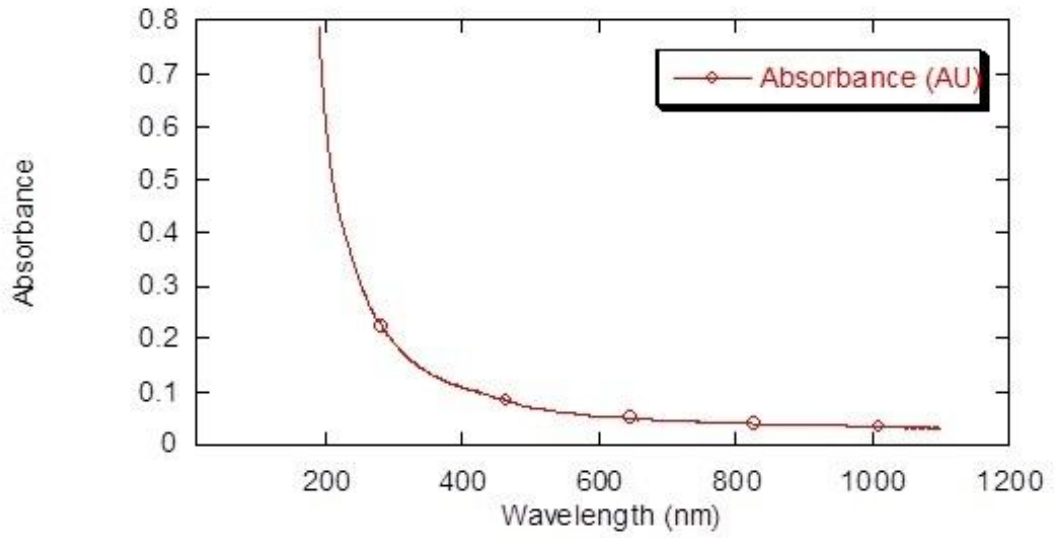

Figure 1: Absorption Spectrum of Type-II CdTe/CdS/ZnS Core/Shell/Shell Qunatum Dots as a Dropast Film

The nanocrystals exhibit multiband absorption spectra with absorption feature up to the near ultra violet range. In nanocrystals the absorption peaks continually red shift (the reduction of optical absorption) and lose their definition with each additional monolayer or capping. In type-II QD's (staggered band alignment) either the valence or the conduction band of the narrow band gap materials lies outside the band gap of the other material, forming an indirect gap in real space, which lowers the energy of photoluminescence (PL) emission as in Figure 2 (a).

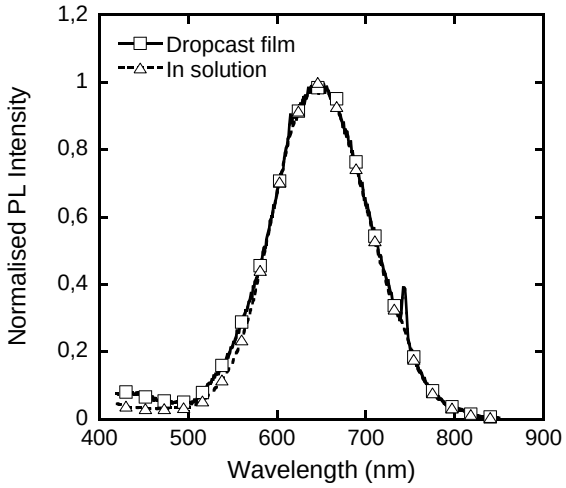

Figure 2(a): Photoluminescence Spectra of CdTe /CdS/ZnS as a Dropcast Film (solid line) and in Solution (Dashed Line)

In this study, we found that the double-capped CdTe yielded featureless absorption spectra. There are several possibilities for the observation (23). The photoluminescence was red-shifted indicating reduction in quantum confinement, with increase in the dot size from 537 nm for capped CdTe to 670 nm for double capped Cds/ZnS CdTe, compared with the previous quantum dot size with a single capping (24). Photoluminescence decay curves allow us to measure the level of wave function overlap of the charge carriers, since according to Balet et al (25) the wave function

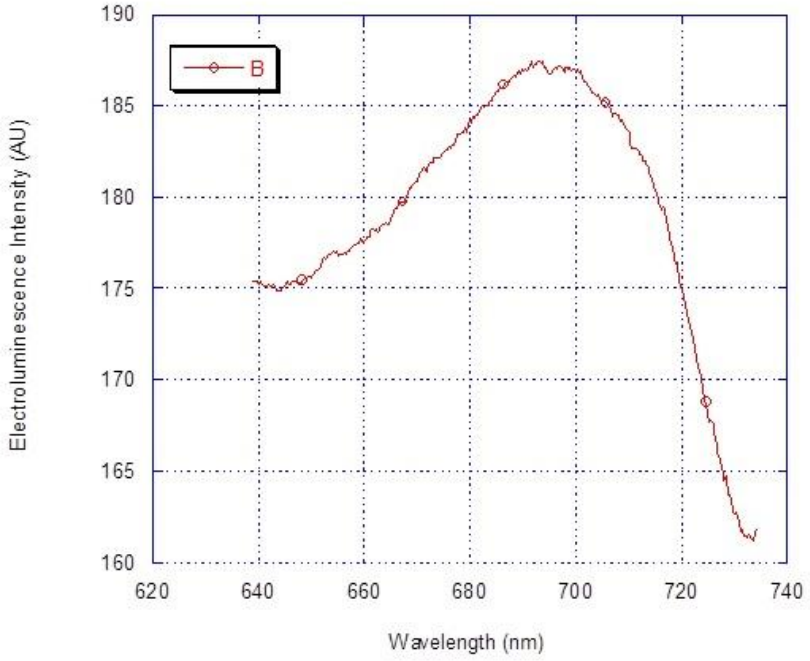

Figure 2(b): Electroluminescence Spectra of CdTe/CdS/ZnS

overlap integral is directly proportional to the radiative lifetime in QD. So with the staggered type-II we should overlap integral is directly proportional to the radiative lifetime in QD. So with the staggered type-II we should expect weaker overlap between the electron and hole due to larger charge separation resulting in longer lifetime values.

The non-exponential trend has frequently been observed for different kinds of II-VI nanocrystals (35) including this work. Recombination carriers from the core/shell -1 and shell-1/shell-2 interfaces are expected to result in the longest lifetime component in the staggered type-II due possibly to fast surface/interface trapping processes as suggested by

Balet et al (25). Our results suggest an increase in the conduction band offset with increase in the shell thickness. A core/shell -1/shell -2 structure exhibited longer lifetimes than core/shell with the same number of shell -1 monolayers (26). This long decay time and the PL red shift with the addition of ZnS shell suggest electron wave function leakage through that shell. The non- exponential (multiexponential) decays in CdTe QDs have been explained in terms of a variation in the non-radiative decay rates caused by trap states (27). A tendency of increase in PL decay times, with increase in size, was observed for II-VI nanocrystals in general (26). In Figure 2(b) the electroluminescence is plotted versus wavelength (nm), where the emission is centered around ≈ 690 nm which is different from the PL spectrum. This is due to the lattice strain similar to the findings of Andrew Smith et al (28) in which the nanocrystalline core is "squeezed" by the double shell CdS/ZnS. This produced the spectral shift(red shift) and extended excited state life time (by 50 μS) as in Figure 2(c). This large mismatch between the core/shell/shell lattice parameters induces strain at the core/shell and shell/shell interfaces (29). It has been reported that shells thicker than ≈2 monolayers will lead to the formation of defects , hence decrease in the quantum yield and the stability (30). The staggered configuration results in a spatial separation of electrons and holes which gives rise to spectral shifting(red shift) towards longer wavelengths (lower energies). Points of evidence for this red shift (the reduction of distinct optical absorption) are featured in Figure 1.

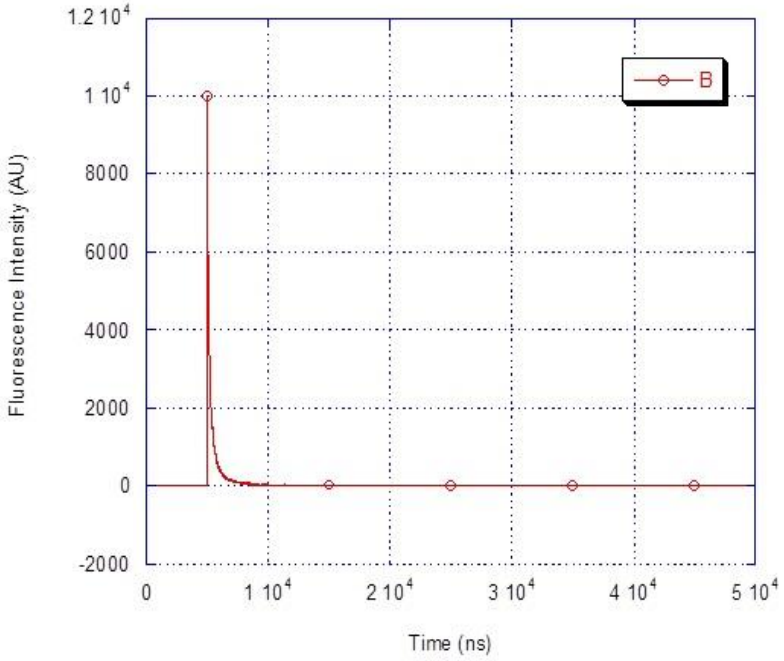

Figure 2(c): Fluorescence Intensity Spectra of CdTe/CdS/ZnS

In Figure.2 (c) a sign of significant increase in excited state life time is exhibited. According to Andrew Smith et al (28) the largest spectral shifts are observed with very small cores such as 1.8 nm CdTe (in our case the core was 3.0 nm CdTe). Kim et al (31) reported that type II colloidal quantum dots can achieve charge carrier separation with staggard band offsets for the core and shell . The current-voltage-luminescence (IVL) behaviour of the devices is shown in Figure 3 where the current and emitted light intensity are plotted as a function of voltage. The curves span a wide range from lower to higher voltages in accordance to the uncontrolled thickness of the CdTe QD layer, which was produced by drop casting on bare oxygen plasma treated ITO. Figures 3 and Figure 4 show a constant trend with regard to the light emission turn on voltage. Depending upon the method of preparation the junction will turn on (liminate) only when the ITO is connected as an anode. When the positive terminal of the voltage source was connected to ITO the light intensity was found to be less compared to when the ITO was connected to the negative terminal. This was the case for the CdTe QD spun on ITO, whilst the drop casting case produced junctions with forward or reverse bias with gentle heating or both. The case which produced luminescence with both signs of bias, but not with the same intensity, is the CdTe spun on ITO with oxygen plasma treatment followed by gentle heating (Figure 5).

In this study there are cases (Figure 3 and Figure 5) similar to those of Hikmet et al (32) on CdSe in which the devices show a small rectification. The light emission bias (Figure 3) was reversed due to the random orientation effect of

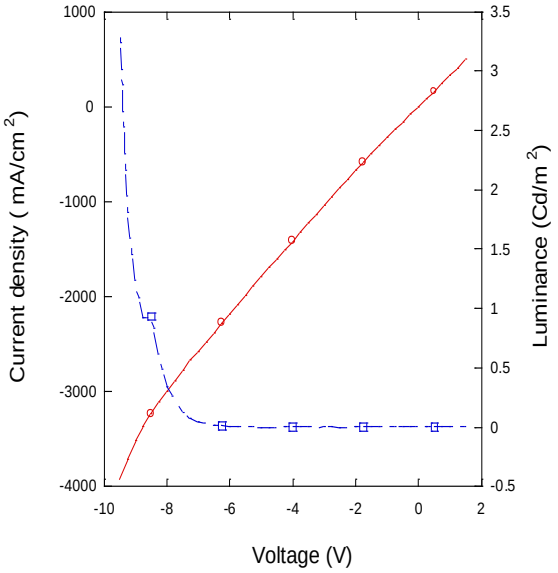

Figure 3: Current-Voltage-Luminance Plot of ITO/CdTe/CdS/ZnS Core/Shell/Shell Quantum Dots/Ca-Al

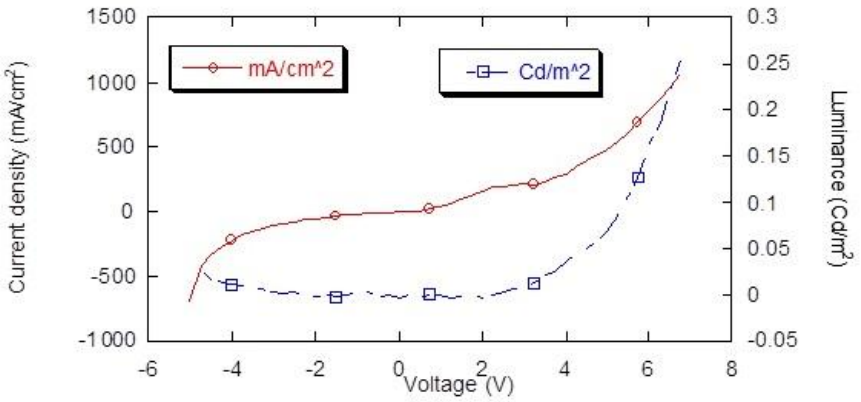

Figure 4: Current-Voltage-Luminance Plot of ITO/ CdTe/CdS/ZnS Core/Shell/Shell Quantum Dots/Ca-Al

heat after the drop casting, which is similar to the behaviour of polarity change of frozen junction (33), but dictated by heating only. The results shown in Figurre 6 are very similar to those by Tesser et al (34). A similar result has been observed in polymer bilayered devices in which the emission produced is from the layer closest to the cathode (35). It is known that prototype semiconductor polymer PPV (poly-para-phenylene-vinylene) screens the real characteristics of the QDs in composite diodes (32). Since the operating voltages (the minimum voltages required) of these devices are lower than for those of PPV alone (with operating voltages of 7 V) , we can expect that the these devices are lower than for those of PPV alone (with operating voltages of 7 V) , we can expect that the electron affinity of CdTe is to be greater than that of PPV. These higher electron affinities decrease the 'turn on voltage' and leads to a build-up of negative charge at the polymer/CdTe interface (16). This may be checked by taking the recombination zone away from the electrodes -1 which otherwise could produce quenching. A feature worth mentioning is that under reverse bias, our samples did not experience dielectric breakdown as in the case reported by Colvin et al (6). The ITO/CdTe QD combination behaved in a

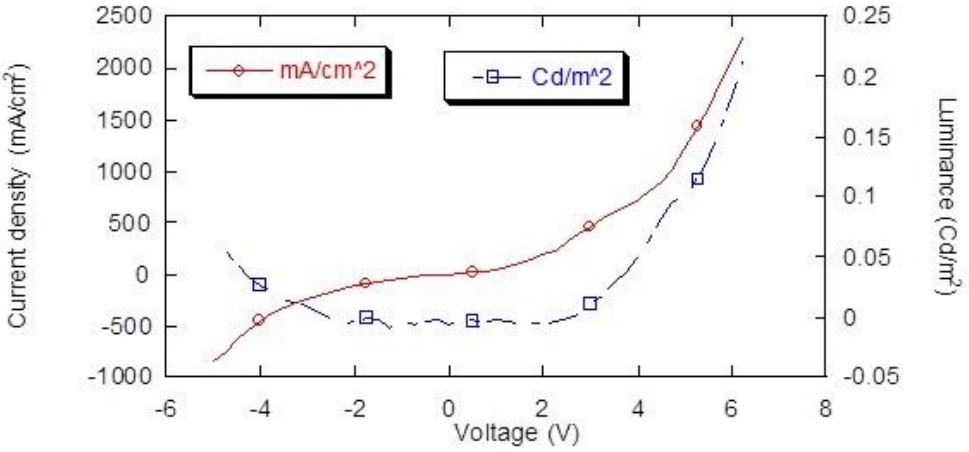

Figure 5: Current-Voltage-Light Plot of ITO/ CdTe/CdS/ZnS Core/Shell/Shell Quantum Dots Spin Coated

manner similar to the PEDOT/CdSe combination (36), i.e. light emission is induced at about 3-4.5 V when driven at positive positive bias and at higher voltage when a negative bias is applied. However, a similar or close value of voltage was observed in positive or negative bias when spin coating was used. Spin coating of CdTe produced reproducible and similar turn on voltages within the experimental error . We noticed from the above mentioned results that the efficiency of luminescence and the 'turn on' voltage depend on how the junction is biased, which clearly indicates that the mechanism at play here is based on injection of holes and electrons into the quantum dots. When the cathode (Ca) is at positive bias, hole injection becomes more difficult as work function of Ca is about 1.8 eV higher than that of ITO. This rather low value for luminescence is due to the fact that the emissive CdTe QD layer is next to the metal electrode, which causes quenching of emission (37). Typical dark current-voltage linear plots are shown in Figure 5. For these diodes diodes the weakly rectifying 'turn on' voltages around 3.5 V were observed.

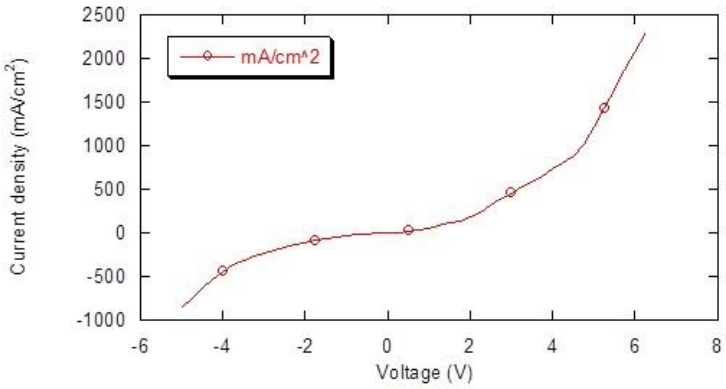

Figure 6: A Current-Voltage Plot of ITO/ CdTe/CdS/ZnS Core/Shell/Shell/Al

The semi-logarithmic plot in Figure 6 of the I-V characteristics, in forward bias for the same diode, illustrate that there are two plateaus in the forward bias I-V curves indicating the deviations from the ideal diode. Under moderate forward bias (between 1 to 2 V) there exists a near linear region. At higher voltages the current seems to saturate, and with the series resistance effect it appears to dominate the conduction process in this regime.

The linear region can assumably be described by the thermionic emission theory, i.e. I = exp(QV/nKT), where 'Q' is the electron charge, 'K' the Boltzmann constant, 'T' the absolute temperature of the diode, and 'n' the diode ideality factor. This feature of the I-V characteristics suggest that the other current transport mechanism is dominant and hence the thermionic emission is suppressed. It may be noted that there is more than one slope in the low, medium and high forward biased regimes (38). This has been oftenly found with nanostructured Schottky devices (39). A linear region in the low forward bias implies a small contribution of surface/interface traps, whereas in the higher forward bias the contribution of the surface/ interface traps to the potential is larger. This was reported for CdSe-ZnS QD's action as the as the deep electron trap (38). The I-V characteristics of these diodes were plotted on a semi-log scale (Figure7) to understand more clearly about their electrical properties. At low voltages an ohmic relationship $I = V^{(m)}$ is observed. At higher voltages the current rises quickly with 'm' between 2 and 22. These phenomena are the characteristics of space charge-limited current conduction.

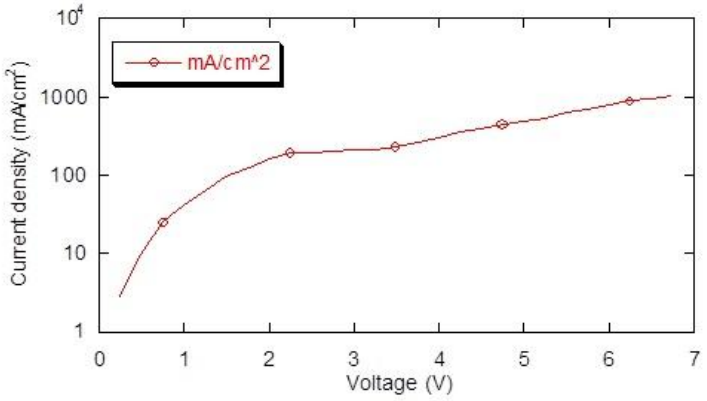

Figure 7: Semi-Logarithmic Current-Voltage Plot of ITO/ CdTeCdS/ZnS Core/Shell/Shell/Al

Further research predicts that improved performance can be achieved by incorporating nanowires or nanorods (CNT or Au rods). The red shift of the electroluminescence (EL) spectrum as compared to the photoluminescence (PL) spectrum is quite common for the nanoparticles (40, 34, 41) and nanorod devices (42). It is attributed to re-absorption of the EL signal within the nanoparticle layer (40), energy transfer from small to big nanoparticles (40, 34), Stark effect from high local fields (43), or local heating due to poor thermal conductivity of the emitting layer (41).The fact that EL (light) is observed in both directions is comparable to light emission from other nanoparticles devices (32). Major difficulties using the solution – synthesized QDs are caused by their organic constituents, the surfactant molecules for surface passivation. The organics must be replaced by the short organic pyridine (which may cause frustrating PL quenching by more than 95 %), or removed during the thin film deposition. This is because they disturb the injection of the high-field accelerated electrons or carriers and degrade the device in operation (44), or create hypervalent surface interactions (45) which can be applied to IV-VI compounds as well as to III-V. This was tested by fabricating Al/Si NC/Al vertical structure recently by O Lopez-Sanchez (46). In this case the Si surface was passivated with hydrogen (47).

In conclusion the nanocrystal based light emitting diode is better made after the reduction or removal of the supporting organic layers.

4. ACKNOWLEDGEMENTS

The most part of this work was competed at University College London. AW thanks Prof. F. Cacill and his group in the technical support and helpful discussion. Thanks are due to his staff for assistance in the preparation of this manuscript. The technical assistance provided by the British Institute of Technology in some respect is also acknowledged with thanks. Authors are indebted to University College London for allowing to utilize the facilities available there.

5. REFERENCES

(1) Talin Ayvazian , Wytze E. Van der Veer , Wendong Xing , Wenbo Yan and Reginald M. Penner ; Am. Chem. Soc. Nano, 7 (10) , pp 9469- 9479, 2013
(2) Yungting Chen , Hanyu Shih , Chenhsiung Wang , Chunyi Hsieh , Chihwi Chen , Yangfang Chen and Taigting Lin ; Optics Express , 19 (S3), pp A319- A325, 2011
(3) Sergio Brovelli , Wan Ki Bae , Christopher Galland , Umberto Giovanella and Victor I. Klimov ; Nano Lett. , 14(2) , pp 486-494, 2014
(4) Jen It Wong , Nimai Mishra , Guichuan Xing , Mingjie Li , Sabyasachi Chakrabortty , Tze Chien Sum , Yumeng Shi , Yinthai Chan and Hui Ying Yang ; Am. Che. Soc. Nano , 8(3) , pp 2873-2879 , 2014
(5) Benjamin S. Mashford , Mathew Stevenson , Zoran Popovic , Charles Hamilton , Zhaoqun Zhou , Craig Breen , Onathan Steckel , Vladimir Bulovic , Moungi Bawendi ,Seth Coe-Sullivan and Peter T. Kazlas ; Nature Photonics , 7, pp 407-412 , 2013
(6) L. Colin ; Nanoarchitured and Nanostructured Materials , Wiley-Vch, Weinheim , 2004
(7) G. Schmid ; Nanoparticles, Wiley, New York, 2004
(8) C. P. Poole and F . I. Owens ; Introduction to Nanotechnology , Wiley , New York , 2003
(9) Murry C. B. , Sun S. , Gaschler W. Doyle H. Bently T. A. And Kagan C. R. ; IBM J. Res. Dev. , 145, pp 47-56 , 2001
(10) V. Schukin , N. Nledentsov and D. Bimberg ; Epitaxy of Nanostructures , Springer , Berlin/ Heidelberg , 2003
(11) Y. Ohno , S. Kishimoto , K. Maezawa and T. Mizutani ; Jpn. J. Appl. Phys. , 40 (3B) , pp 2065-2068 , 2001
(12) H. Chu and C. P. Liu ; App. Phys. Lett. , 89 , 82- 105, 2006
(13) Gao C. Lesser , S. Kristein and H. Mohwald ; J. Appl. Phys. , 87 (5) , pp 2297-2302 , 2007
(14) Pileni M. P. ; Today , 58, p151 (abstract) , 2000
(15) Morgan N. Y. Leatherdale C. A. , Drndic M. , Jarosz M. V. , Kastner and M. A. Bawendi ; Phy. Review B 66, pp 3391-3399, 2002
(16) Green M. , Harwood H., Barrowman C. , Rahman P. , Eggeman A. , Festry F. , Dobson P. ,and Nigal T. ; J. Matter Chem. ,17, pp 1989- 1994, 2007
(17) Shu-Hsien Wu , Yue Kuo and Chi-Chou Lin ; MRS Proceedings, pp 199-204 , 2012
(18) Yuki Tani , Satoshi Kobayashi and Hiroshi Kawazoe ; MRS Proceedings , pp 107- 122, 2007
(19) Jiangxin Wang , Chaoyi Yan , Shlomo Magdassi and Pool See Lee ; ACS Appl. Material Interfaces , 5(15) , pp 6793-6796 , 2013
(20) Rebecca J. Anthony , Kai-Yuan Cheng , Zachary C. Holman , Russell J. Holmes and Uwe R. Kortshagen ; Nano Lett. , 12(6) , pp 2822-2825, 2012
(21) Coe-Sullivan , S. Woo , W. K. Steckel , J.S. , Bawendi M. And Bulovic V. ; Org. Electron , 4, pp 123-130, 2003
(22) Gaponenko S. V. , Kapitonov A. M. , Bogomolov A.V. , Prokofiev A.V. , Eychmuller A. And Rogach A.L. ; JETP Lett. , 68 (2), pp 142-147, 2011
(23) Tonti D.V. , Vanmourik F. and Chergi M. ; Nano Lett. 4, pp 38-44, 2004
(24) J. Zhao , J. Zhang , C. Jiang, J. Bohnenberger , T. Basche and A. Mews ; J. Appl. Phys. , 96 (6), pp 3206-3210, 2003
(25) Balet. L. , P. Ivanov S.A. , Piryantinski A. , Chemann M.A. and Klimov V. : Nano Lett. 4, pp1485- 1490, 2004
(26) Crookers S.A. , Hollingsworth J.A. , Tretaik S. and Klimov V. ; Phys. Rev. Lett, 89, 1868- 1872, 2002
(27) Wang X.. Qu. L., Zhang J. , Peng X. , and Xia M. ; Nano Lett. 3, pp 1103-1107, 2003
(28) Andrew M. Smith and Shuming Nie ; Nature nanotechnology, 14, pp 56-63, 2009
(29) C. G. Donega, P. Lijeroth and D. Vanmaeberg ; Small Tech. , 12 , pp 1152-1162, 2005
(30) D. Talapin, I. Mekis, S. Gotzinger, A. Komowski, O. Benson and H. Willer, J. Phys. Chem. B 108, pp 1882-1892, 2004
(31) S. Kim, B. Fisher and H. J. Bawendi ; J. Am. Chem. Soc., 125, pp 114-126, 2003
(32) Hikmet R. A. M. , Talapin D. V. And Weller H. ; J. Appl. Phys. , 93, 3509- 3514, 2003
(33) Gao J. , YU G. and Heegan J. ; Appl. Phys. Lett. , 71 (10), pp 1293- 1295, 2000
(34) Tesster N. , Medvedev V. , Kazes M. , Kan S. and Banin U. ; Science, 295, pp 1506-1508, 2002
(35) Q. Sun, Y. Li and Q. Pei ; J. Display Tech. , 3 (2), pp 211-224, 2007
(36) Y. Li, A. Rizzo, M. Mazzo, L. Carbone, L. Manna, R. Cingolani and G. Gigli ; J. Appl. Phys. , 97, pp 11350-11361, 2005
(37) Chen C. Y., Cheng C. T., Yu J. K., Pu S. C., Cheng Y. M., Chai P. T., Chou Y. H. and Chiu H. T. ; J. Phy. Chem. , B 108, pp 1068- 1077, 2004
(38) J. M. Caruge, J. E. Halper, V. Wood, V. Bulovic and M. G. Bawendi ; Nature Photonic , 2, pp 247-250, 2008
(39) N. Arpatuznis, D.H. Tassis, C.A. Dimitriadis, C. Chaitidis, J. D. Song , W. J. Choi and J. I. Lee ; Semicond. Sci. Tech. , 22, pp 1068-1091, 2007

(40) M. C. Schlamp, X. Peng and A. P. Alivisatos ; J. Appl. Phys., 82, pp 5837- 5842, 1997
(41) J. Huang, Y. Yang, S. Xue, B. Yang and J. She ; Appl. Phys. Lett. , 70, pp 2335-2342, 1997
(42) R. Konenkamp, R.C. Word and M. Godinez ; Nao Lett. , 5 , pp 2005-2012, 2005
(43) J. M. Caruge, J. E. Halpert, V. Bulovic and M. G. Bawendi ; Nano Lett. , 6, pp 2991-2998, 2006
(44) Y. Tani , S. Kobayashi and H. Kawazoe ; J. Vac. Sci., Tech., A 26 (4) , pp 1058-1061, 2008
(45) L.M. Wheeler, N. R. Neale, T. Chen and U. Kortshagen ; Nature Communications, 31, pp 1-10, 2013
(46) O. Lopez- Sanchez ; Ame. Chem. Soc. Nano, 18(3), pp 3042-3048, 2014
(47) Takahagi T., Nagai I. , Ishitani A. Kuroda H. and Nagasawa Y. ; J. App Phys. , 64, pp 3516- 3521, 1988

.